PHYSICAL REVIEW B VOLUME 32, NUMBER 10 15 NOVEMBER 1985

Particle motion in a mixed dynamic alloy: Binary system in one dimension

R. A. Tahir-Kheli and Nagwa El-Meshad
Department of Physics, Temple University, Philadelphia, Pennsylvania 19122
(Received 21 January 1985)

The long-time dynamics of labeled particle motion in a mixed, random dynamic binary alloy composed of a minimally interacting lattice gas are investigated by the use of precision Monte Carlo simulations. For the mean-square displacement, the results corroborate the theoretical predictions of Tahir-Kheli. With the use of scaling arguments, the theoretical expressions given by Levitt for a single-component system are generalized to a multicomponent format. The predictions of such a scaling procedure for the long-time limit of the space- and time-dependent distribution function are tested in detail against the corresponding Monte Carlo results. Again, very good overall agreement is found between the two sets of results.

I. INTRODUCTION

This is the third in a series of papers[1,2] concerning particle diffusion in minimally interacting (MI) concentrated dynamic lattice gases with spatial anisotropy and constituent mixing. More precisely, paper I dealt with self-diffusion in the two-dimensional isotropic and anisotropic MI systems,[1] whereas paper II analyzed the A- and B-particle diffusion in a mixed A-B alloy, composed of a MI lattice gas, in two and three dimensions.[2]

The present paper differs from I and II in several aspects. First, it refers to one dimension which does not admit diffusion of the labeled atoms. Second, while in papers I and II only the mean-square displacements of the labeled particles were analyzed, here we also examine their space- and time-dependent correlation function (to be referred to as the "distribution function").

Another class of distinctions between this and the preceding work pertains to paper II. Both this paper and II deal with a mixed binary alloy consisting of dynamic MI lattice gases. What is different here is that unlike in two and three dimensions, the theoretical situation in one dimension is relatively clean. Here the long-time characteristics of the mean-square displacement of a labeled tracer, which is otherwise identical to the background atoms, have been well established in many studies.[3–6] Even the corresponding properties of a tracer which is arbitrarily different from the background have been predicted.[7] Most important of all, there is a prediction[8] of the long-time behavior of the mean-square displacement of an arbitrary tracer hopping through a multicomponent dynamic background which is expected to be valid in the limit $J^0\tau\rightarrow\infty$ (here, J^0 is the hopping rate of the tracer).

With this as the background, one might erroneously conclude that a Monte Carlo simulation is hardly necessary since the theory is all in place. That this is not so becomes clear if we also consider the time- and space-dependent distribution function. While Levitt's theory provides a firm basis for the distribution function in single-component alloys involving a designated tracer with an identical background (also compare the corresponding Monte Carlo simulations for this case,[9] no such work relating to multicomponent alloys is available. Accordingly, in this paper we present reasonable scaling arguments which help extend Levitt's single-component distribution function to a more general case. To test this scaling conjecture, an extensive set of Monte Carlo simulations are undertaken which, as a by-product, also provide a corroboration of Tahir-Kheli's prediction of the mean-square displacements in such a multicomponent alloy. Our Monte Carlo results indicate the scaling conjecture to be correct.

II. SIMULATION PROCEDURE

The well-known simulation procedure for a single-component one-dimensional MI system[6] is first extended to deal with the case of two-component alloys with macroscopic concentrations c^A and c^B and hopping rates J^A and $J^B=\eta J^A$ ($\eta\leq 1$). It is convenient to also give a brief description of the essential steps below:

(0) Choose a lattice consisting of a suitably large number N of sites. Impose periodic boundary conditions by following the usual regimen. Also assign another column matrix with N_A+N_B elements where the actual locations (not subject to periodic boundary conditions) of the atoms can be stored.

(1) Randomly distribute $N_A=Nc^A$ and $N_B=Nc^B$ atoms of varieties A and B, respectively. (The identity of these atoms can be coded by assigning the site-occupancy variable to be equal to 1, for an A atom, -1 for a B atom, and 0 for a vacancy.)

(2) Randomly choose one of the $N'=N_A+N_B$ atoms as the candidate for a possible hop.

(3) Check for the identity of the chosen atom. If it is an atom of species A, proceed to step (4), but if on the other hand the chosen atom is of variety B, call a real random number r, evenly distributed between zero and one,

to see whether it is less or more than the predetermined ratio η. If $r<\eta$, the control passes to the subsequent command [(4) below]; otherwise, it returns to step (2).

(4) Once we get to this point, the remainder of the code if similar to that used previously.[6] We now toss a coin to decide whether the chosen atom is to move in the positive or negative directions. When this is done, we check to see whether the site to which the intended hop will take the given atom is empty or occupied. Of course, if the relevant site is occupied, we leave the chosen atom in its current location and go to statement (5) below. On the other hand, if the site for the intended hop is empty, we move the particle to this site and upgrade the coordinate of the particle to reflect its new location.

(5) The control is once again returned to command (2) above to select yet another candidate for hopping.

(6) The above operations, i.e., (2)—(5), are repeated until a total of N' candidates for hopping have been processed.

The procedure outlined in steps (2)—(6) inclusive constitutes *a single Monte Carlo step per atom* (MCS/p). We now repeat this entire process a total of τ number of times (i.e., for τ MCS/p). Knowing the original as well as the final locations (after time τ) of all the N' particles on the unbounded shadow lattice, we can readily calculate the mean-square displacements for the A, i.e., X_A^2; the B, i.e., X_B^2; or an average particle $\langle X^2\rangle_{(\tau)}$.

III. ANALYSIS

Before we proceed to the description of the results, a few words regarding the analysis are in order. Once the data for the mean-square displacement $\langle X^2\rangle_{(\tau)}$ and the distribution function have been accumulated, their analysis is focused at two complementary objectives.

First, we attempt to establish the asymptotic time dependence of $\langle X^2\rangle_{(\tau)}$ to check whether it has indeed developed the $t^{1/2}$ character.[1-6] In other words, we check first for the adequacy of the relationship

$$\langle X^2\rangle_{(\tau)}=B_0\tau^{\mu},\quad \mu=\tfrac{1}{2},\quad \tau\to\infty\ . \tag{3.1}$$

This is a relatively simple task in that we plot $\log_{10}\langle X^2\rangle_{(\tau)}$ versus $\log_{10}(\tau)$ and look for a straight line with slope $\mu=0.5$ to appear in the late stages. Depending on the value of η, the simulations were run between $\tau=0$ and $\tau_{\max}$, where $\tau_{\max}$ ranged between 10 000 and 38 000 MCS/p). This check is useful in helping to choose an appropriate $\tau_{\max}$ such that an extended span of time is available over which (3.1) fully obtains.

The achievement of the second goal requires more effort. Here, we attempt to compute the Tahir-Kheli collective hopping rate $\tilde{J}$ and compare it with the parameter-free prediction given in Eq. 17 of Ref. 6.

To this end, we proceed as follows: For finite MCS/p times τ_0 and τ, where

$$\tau>\tau_0\ \text{ and }\ \tau_0\gg 1\ , \tag{3.2}$$

we write

$$\langle X^2\rangle_{\tau}=B_0\tau_0^{1/2}+c_1+O(\tau_0)^{-1/2}\ , \tag{3.3}$$

$$\langle X^2\rangle_{\tau}=B_0\tau^{1/2}+c_1+O(\tau)^{-1/2}\ . \tag{3.4}$$

These in turn give

$$(\langle X^2\rangle_{\tau}-\langle X^2\rangle_{\tau_0})/(\tau^{1/2}-\tau_0^{1/2})=B_0(\tau_0)+R\ . \tag{3.5}$$

For large enough τ_0, the remainder R can be neglected. Therefore, we choose an appropriately large value for the starting time τ_0. Next, the slope B_0 is computed using Eq. (3.5) by setting $R=0$. This slope B_0 is clearly a function of both τ_0 and τ.

In order to exploit the data to their fullest, we compute the slope $B_0(\tau_0)$ for all the times $\tau>\tau_0$ (note, the data are collected in varying intervals of 10 to 1000 MCS/p each) and then average the result over the set of values τ used. In this fashion, we get our best result for the slope $\bar{B}_0(\tau_0)$. Next, the starting time τ_0 is increased to the next available (higher) time τ_1, and the entire process is repeated to obtain the slope $\bar{B}_0(\tau_1)$. This procedure is continued until we obtain $\bar{B}_0(\tau_m)$, where the maximum time τ_m is so chosen that at least ten more points for the data $\langle X^2\rangle_{(\tau)}$ vs τ are still available.

The final best estimate for the slope $\bar{B}_0$ is now computed in the usual manner by determining the overall average of the various mini averages $\bar{B}_0(\tau_i)$, i.e.,

$$\bar{B}_0=\sum_{i=0}^{M}\bar{B}_0(\tau_i)/(m+1)\ . \tag{3.6}$$

Two issues still need to be resolved. Firstly, the magnitude of the expected error in the "best" estimate for the slope $\bar{B}_0$ has to be specified. Secondly, the procedure for converting this number into a well-defined relationship for checking the Tahir-Kheli (TK) predictions needs to be spelled out in precise terms.

Regarding the error in $\bar{B}_0$, we might anticipate it to be of the order of the root-mean-square deviation Δ, where

$$\Delta^2=\sum_i[\bar{B}_0(\tau_i)-\bar{B}_0]^2/(m+1)\ . \tag{3.7}$$

It turns out, however, that in every instance the quantity Δ so estimated is larger than the "actual error." The "actual error" is, of course, trivial to calculate because TK's theoretical result for the slope $\bar{B}_0$ is

$$\bar{B}_0(\mathrm{TK})=[2(1-c)/c^{1/2}]a^2(\tilde{J}/\pi)^{1/2}\ , \tag{3.8}$$

where

$$\tilde{J}=\left[\sum_{\lambda}c^{\lambda}/J^{\lambda}\right]^{-1}\ . \tag{3.9}$$

The second issue to be resolved relates the magnitudes of the hopping rates J^A and J^B. It is clear from the description of the simulation procedure that for the A atoms, the hopping rate J^A, in units of $(\mathrm{MCS}/p)^{-1}$, is equal to one-half. The J^B, on the other hand, is related to J^A through the parameter η and therefore

$$J^B=\eta/2\ \ (\mathrm{MCS}/p)^{-1}\ . \tag{3.10}$$

We have analyzed one grand sample (GS) consisting of $N_G\sim 500\,000$ particles with the ratio $\eta=0.5$ and three different similarly large GS's with $\eta=0.1$. The concentrations c^A and c^B were chosen to lie outside any perturbative regimes. For instance, for GS-I, $c^A=c^B=\frac{1}{4}$, and

for GS-II, GS-III, and GS-IV, we chose, respectively, $c^A=c^B=\frac{1}{4}$; $c^A=\frac{1}{6}$, $c^B=\frac{1}{3}$; and $c^A=\frac{1}{3}$, $c^B=\frac{1}{6}$. These four GS's comprised 40—45 mini samples, each with 24 000 sites and approximately 12 000 particles (that is, $N^A+N^B\sim 12\,000$). To get good statistics for the long-time behavior, we ran the GS-I for 10 000 MCS/p and the GS-II—GS-IV were each run for up to 15 000 MCS/p.

For the most extreme case analyzed, for which the hopping rate of the slower B atoms was fully 100 times smaller than that of the faster atoms, we worked with a larger GS. Here we averaged over a total of 60 different mini samples, thus totaling $N_G\sim 0.72\times 10^6$ particles. Moreover, in order to wait long enough for all the particles to fully reach their asymptotic behavior, we had to run the GS-V for 38 000 MCS/p.

IV. RESULTS: THE MEAN-SQUARE DISPLACEMENT

In Table I we have listed both the theoretical and the numerical simulation estimates for the slope $\bar{B}_0$. In addition, also listed are the theoretical results for the TK effective hopping rate $\tilde{J}$ and the corresponding simulation estimates (note that the simulation estimates for $\tilde{J}$ are obtained indirectly from the slope $\bar{B}_0$).

It is observed from Table I that the values for GS-IV, representing the case $\eta=0.1$, $c^A\sim\frac{1}{3}$, and $c^B\sim\frac{1}{6}$, are the most divergent of all cases studied. Other than being a random happenstance, we have found no satisfactory explanation for this behavior.

The overall agreement between the theory and the simulations for the GS-I is of the order of three parts in a thousand. This level of accuracy is close to the best expected precision of our simulations with $N_G\sim 0.5\times 10^6$ atoms. On the other hand, since η is only $\frac{1}{2}$ and because the Tahir-Kheli theories for the mixed systems are reasonably accurate for $\eta=\frac{1}{2}$, even in two and three dimensions (see paper II), we should not make too much of this rather excellent agreement.

On the other hand, in contrast with $\eta=\frac{1}{2}$, because the ratio $\frac{1}{10}$ lies below even the factor $(1/z)^3$, the case $\eta=\frac{1}{10}$ provides a fairly stringent test of the theory. Again, in order to stay away from the perturbatively accessible concentration limits, our choice of $c^A+c^B\sim\frac{1}{2}$ specifies a suitably nonperturbative concentration regime (especially since both c^A and c^B are also chosen to be approximately of the same magnitude).

For $\eta=\frac{1}{10}$, the simulation and the theoretical results for the three GS's analyzed in Table I are in mutual agreement to an average accuracy of the order of a percent. In particular, if we exclude the inaccordant sample GS-IV, the mutual agreement is again excellent. Indeed, the agreement is of comparable accuracy to that found for the case $\eta=\frac{1}{2}$. Accordingly, the $\eta=\frac{1}{10}$ observations have to be treated as providing a reasonable corroboration of the theory.

We examine next the GS-V, where $\eta=\frac{1}{100}$. Despite the fact that the overall size of this sample was larger, $N_G\sim 0.72\times 10^6$ particles, and the simulations were run for extended times (38 000 MCS/p), this is a difficult system to study by numerical methods. Some of the practical difficulties are self-evident. For instance, the fluctuations in the mean-square displacement of the fast particles are large, depending sensitively on the particular set of configurations in which the slow particles (which act as obstacles to their movement) are distributed. On the other hand, there are other equally significant difficulties intrinsically associated with this simulation which are more subtle to comprehend. An example of this class of difficulties is the following.

In GS-V, a labeled slow particle is in an environment where half the background is composed of highly mobile fast particles. These particles make, on the average, a hundred different hops during the period for one elementary hop by the slow particle. Thus, the single-file aspect for the slow atom in question is considerably vitiated as regards the contribution from the fast background. Indeed, the relative contribution of the fast background is almost mean-field-like to the motion of the slow tracer[7] and, as is well known, the mean-field motion is Einsteinian, leading to a linear contribution to the mean-square displacement of the slow particle. Thus, the slow particles show a quasilinear τ-dependent behavior.

Clearly, this anomalous contribution is an intermediate-time domain effect, disappearing in the limit of truly long times over which the single-file nature of the one-dimensional motion becomes fully apparent. Nevertheless, because from the perspective of the slow

TABLE I. Precision simulation results for the slope B_0, as well as the effective hopping rate $\tilde{J}$, are compared with Tahir-Kheli's theory. These results were obtained from large effective samples [$N_G\sim(0.5$—$0.7)\times 10^6$ particles]. Notice the percentage error in $\tilde{J}$ is twice that in B_0. This merely reflects the relationship $\tilde{J}\propto(B_0)^2$.

GS	η	c^A	c^B	$\bar{B}_0$ (Simulation)	$\bar{B}_0$ (TK theory)	$\tilde{J}$ (Simulation)	$\tilde{J}$ (TK theory)
I	0.5	0.2500	0.2500	0.651±0.002	0.6515	0.666±0.004	0.6667
II	0.1	0.2500	0.2500	0.342±0.002	0.3402	0.184±0.002	0.1818
III	0.1	$\frac{1}{6}$	$\frac{1}{3}$	0.303±0.002	0.3016	0.144±0.002	0.1429
IV	0.1	$\frac{1}{3}$	$\frac{1}{6}$	0.407±0.001	0.3989	0.260±0.001	0.2500
V	0.01	0.2500	0.2500	0.115±0.003	0.1123	0.0208±0.0011	0.0198

tracer, the elapsed time (measured in units of its own hops) is not inordinately *long*, even after 38 000 MCS/p have elapsed; therefore in practice, remnants of the anomalous linear time-dependent terms are not entirely erased. Such unwanted "dominant" interference, from terms whose coefficients are admittedly both small and decreasing in magnitude, would still have a net effect of raising the apparent magnitude of the slope of the proper $t^{1/2}$ term. Given the limitations on the available computer time, the simulation estimates of the slope, 0.115, is in fair agreement with the theory, i.e., 0.1123. (See Table I.)

As mentioned earlier, the case of $\eta=\frac{1}{100}$ is important in that it lies totally outside those regions that can possibly have perturbative solutions. Consequently, the agreement noted above fairly leads to the conclusion that the TK predictions given in Eqs. (3.8) and (3.9) are reasonably well corroborated.

To round off this discussion, we append Figs. 1 and 2 where the simulation estimates for the effective hopping rate $\tilde{J}$ (given as crosses or solid circles) are compared with the corresponding theoretical results[8] (given as solid curves). The solid circles represent the large GS simulation results given in Table I which have already been discussed above. On the other hand, the crosses indicate less accurate results obtained from simulations using mini-grand samples (totaling approximately 48 000—60 000 particles each).

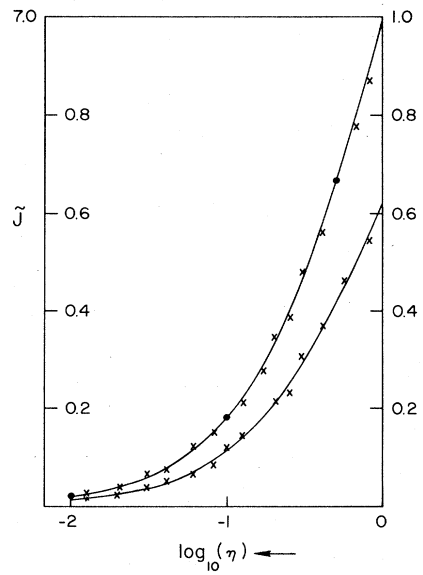

FIG. 1. Tahir-Kheli's collective hopping rate $\tilde{J}$ (solid curves) is compared with our simulation results. We have plotted $\tilde{J}$ as a function of the logarithm of the ratio η. The upper curve refers to the case $c^A=c^B=0.25$, whereas for the lower curve, $c^A=c^B=0.4$. The crosses represent the results obtained from less accurate mini-grand-sample (MGS) simulations, whereas the solid circles represent the precision large GS simulation results.

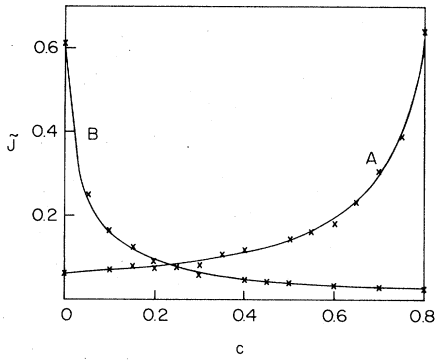

FIG. 2. Collective hopping rate $\tilde{J}$ is given as a function of the concentration of the background particles. For curve A, $\eta=0.1$ and the abscissa represents c^A, whereas for curve B, $\eta=0.04$ and the abscissa measures c^B. The TK theoretical predictions are given as solid curves, whereas the crosses are obtained from our simulations on MGS.

V. PROBABILITY DISTRIBUTION FUNCTION

As noted in Ref. 8, in one dimension there appears to exist a natural correspondence between the multicomponent and the single-component systems. Through the transformation suggested by Tahir-Kheli,[8] the dynamical properties of an average atom in a multicomponent system can be represented much like those of the single-component system. This transformation consists in defining an "effective background" of an equivalent single species of atoms. The effective concentration of such a background is the *sum* of the concentrations of all the various species that constituted the background in the original, multicomponent alloy. Moreover, the effective hopping $\tilde{J}$ is given by the relation (3.9), intrinsic to which is the inverse weighting factor which assigns higher relative importance to the slower atoms in the background.

In view of this correspondence, it is natural to propose a new extension of the theory which predicts the behavior of the space- and time-dependent distribution function in the multicomponent system. To this end, let us rewrite Levitt's formula for the distribution function $P(X,t)$ of a single-component system, i.e.,

$$P(X,t)=[2\pi\alpha(t)]^{-1/2}\{\exp[-X^2/2\alpha(t)]\} . \tag{5.1}$$

In precise terms, the significance of the function $P(X,t)$ is the following: Given a labeled atom at position zero at time zero, the probability that after time t the same atom will be found at position X is $P(X,t)$. Accordingly, the distribution function obeys the following two conditions:

$$P(X,t)=\delta(X) \quad \text{for } t=0 ,$$

$$\int_{-\infty}^{\infty} P(X,t)dX=1 \quad \text{for all } t .$$

The above conditions lead to the result

$$\langle X^2\rangle_{(t)}\equiv \int_{-\infty}^{\infty} P(X,t)X^2dX=\alpha(t) . \tag{5.2}$$

Because the distribution function of necessity relates to a given labeled atom, for the general system it must de-

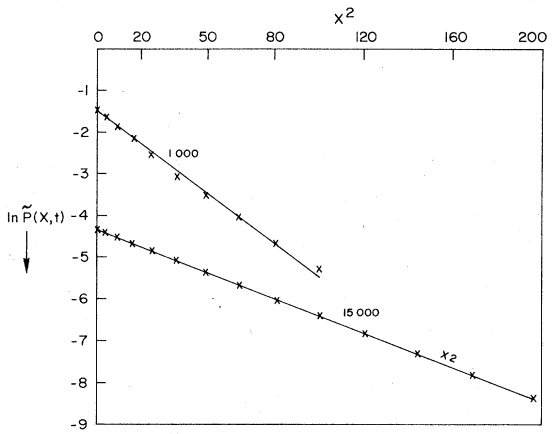

FIG. 3. Logarithm of the total distribution function $P(X,t)$ is plotted as a function of the square of the displacement X^2. The solid lines represent the results of the scaling conjecture. The corresponding times t are noted above the curves. The crosses display our simulations. Here the ratio $\eta=0.1$ and $c^A=\frac{1}{3}$, $c^B=\frac{1}{6}$. These simulations were carried out on large GS.

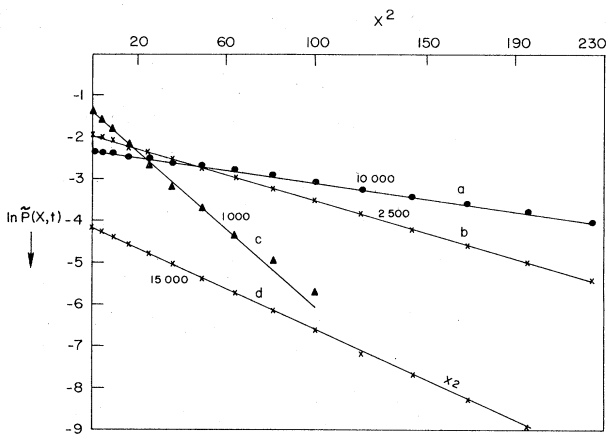

FIG. 5. Similar to Figs. 3 and 4. Here curves a and b refer to the case $\eta=0.5$ and $c^A=c^B=0.25$. The relevant times are recorded above the curves which are, in fact, straight lines. For curves c and d, $\eta=0.1$, and $c^A=c^B=0.25$. Again, the ordinate scale for the curve d is twice that shown.

pend on the actual species, say λ, of the atom in question. Thus, we have different distribution functions $P^\lambda(X,t)$ for the different species. Accordingly, the distribution function for the effective system is the weighted average of these functions, i.e.,

$$\tilde{P}(X,t)=\sum_\lambda c^\lambda P^\lambda(X,t)/c \ , \tag{5.3}$$

where $c=\sum_\lambda c^\lambda$.

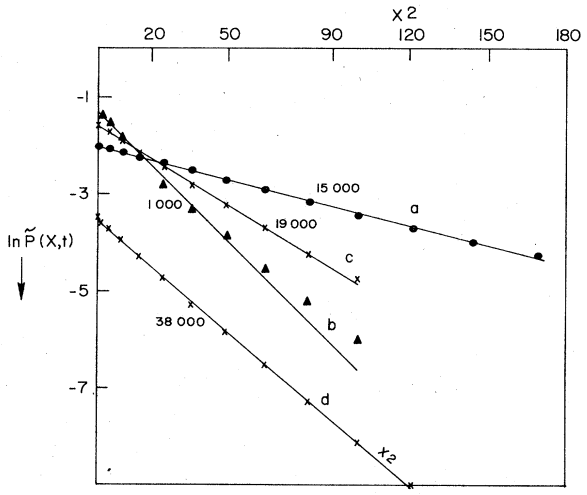

FIG. 4. Similar to Fig. 3 with the difference that η for th curves a and b equals 0.1, while $c^A=\frac{1}{6}$, $c^B=\frac{1}{3}$. For curves and d, $\eta=0.01$ and $c^A=c^B=0.25$. For the curve d the ordinate scale should be read as twice that shown. The various symbols (solid circles, solid triangles, and crosses) display our simulations.

The counterpart of the mean-square displacement for the effective background has already been made precise in the preceding section. It is the average displacement over all the $N'=cN$ particles present. Indeed, in analogy with Eq. (5.3) we can write

$$\langle X^2\rangle_{(t)}=\tilde{\alpha}(t)=\sum_\lambda c^\lambda\langle X_\lambda^2\rangle_{(t)}/c \ , \tag{5.4}$$

where $\langle X_\lambda^2\rangle_{(t)}$ is the mean-square displacement of atoms of the λ species. Therefore, in complete analogy with Eq. (5.1) we get

$$P(X,t)=[2\pi\tilde{\alpha}(t)]^{-1/2}\{\exp[-X^2/2\tilde{\alpha}(t)]\}, \quad \tilde{J}t\gg 1 \tag{5.5}$$

where

$$\tilde{\alpha}(t)=[2(1-c)/c^{1/2}][\tilde{J}t/\pi]^{1/2} \ . \tag{5.6}$$

Although eminently reasonable, the above relationship has been derived only on the basis of a scaling hypothesis. As such, we shall call it a scaling "conjecture."

To test this conjecture, in Figs. 3–5 we have plotted the simulation results of $P(X,t)$ versus the conjectured scaling results given in Eqs. (5.5) and (5.6). It is clear that for long times (to which the conjecture is meant to apply), the fits are excellent. Even for intermediate times, the agreement between the simulations and the theory is reasonable, as long as the relevant X^2 is not much larger than the corresponding mean-square displacement $\alpha(t)$.

VI. CONCLUDING REMARKS

In conclusion, therefore, the following remarks can reasonably be made. In the limit of long times:

(i) Tahir-Kheli's predictions involving a single effective hopping rate $\tilde{J}$ are in excellent agreement with the simula-

tion results for the mean-square displacement in a binary, dynamic MI lattice gas.

(ii) Moreover, this effective background concept lends itself naturally to further generalization. Here, a scaling conjecture regarding the average probability distribution of atoms comprising the multicomponent system relates it to the corresponding mean-square displacement in complete analogy with Levitt's work on a single-component system. The resultant relationship is found to be obeyed to a high degree of accuracy, thus providing a consistent picture of the dynamics of a minimally interacting, one-dimensional, multicomponent system.

ACKNOWLEDGMENTS

This work has been supported in major part by a grant from the National Science Foundation. Partial support from the Temple University Research Incentive Fund is also acknowledged. The authors are greatly indebted to Dr. K. W. Kehr, who motivated this study and offered valuable insights for its execution.

---

[1]R. A. Tahir-Kheli and Nagwa El-Meshad, this issue, Phys. Rev. B **32**, 6166 (1985).

[2]Nagwa El-Meshad and R. A. Tahir-Kheli, preceding paper, Phys. Rev. B **32**, 6176 (1985).

[3]D. G. Levitt, Phys. Rev. A **8**, 3050 (1973).

[4]P. M. Richards, Phys. Rev. B **16**, 1393 (1977).

[5]P. M. Fedders, Phys. Rev. B **17**, 40 (1978).

[6]H. van Beijeren, K. W. Kehr, and R. Kutner, Phys. Rev. B **28**, 5711 (1983).

[7]R. A. Tahir-Kheli and N. El-Meshad, Phys. Rev. B **27**, 7759 (1983).

[8]R. A. Tahir-Kheli, Phys. Rev. B **28**, 2257 (1983).

[9]K. W. Kehr, N. El-Meshad, and R. A. Tahir-Kheli (unpublished).